Molecular orientation and optical anisotropy induced by the stretching of poly(vinyl alcohol)/poly(*N*-vinyl pyrrolidone) blends

Yoshiyuki Nishio* and Hidematsu Suzuki
Faculty of Engineering, Nagaoka University of Technology, Kamitomioka 1603-1, Nagaoka, Niigata 940-21, Japan

and Kazuyuki Sato
Faculty of Engineering, Fukui University, Bunkyo 3-9-1, Fukui 910, Japan
(Received 10 May 1993; revised 14 June 1993)

The polymer pair, poly(vinyl alcohol)/(*N*-vinyl pyrrolidone) (PVA/PVP), is thermodynamically miscible in the amorphous state, as judged from the detection of a single T_g, which is situated between the T_gs of the two homopolymers, over the whole range of compositions of the binary blend. The molecular orientation and optical anisotropy induced by uniaxial deformation of the polymer blends were characterized through fluorescence polarization and birefringence measurements. Two series of samples, designated as PVA/PVP-H and PVA/PVP-L, were examined; these were cast as films from aqueous polymer solutions containing a slight amount of a stilbene derivative as a fluorescent probe (the notations H and L indicate whether the molecular weight of the PVP is much higher or lower than that of the PVA). In both series of blends, development of the molecular orientation in the drawn films became gradually suppressed with increasing PVP content. PVA/PVP-H blends acquired a higher orientation than the corresponding PVA/PVP-L blends with the same composition. The optical birefringence of the oriented films, when compared at a given draw ratio for a series of blends, decreased drastically with an increase in the PVP fraction and eventually changed from positive to negative values at a certain fraction. The critical PVP fraction was much lower in the PVA/PVP-H series than in the corresponding series. An explanation for this is presented in terms of an effect of birefringence compensation, due to the positive and negative contributions of oriented PVA and PVP, respectively. The molecular weight dependence of the segmental relaxation of PVP chains in the drawing process and that of the frequency of interpolymer interactions are taken into account in the discussion.

(Keywords: PVA/PVP blends; molecular orientation; optical anisotropy)

INTRODUCTION

Polymer–polymer miscibility has been investigated for a large number of blending pairs over the past few years. In the course of this extensive work, it has been elucidated that a specific intermolecular interaction such as hydrogen bonding, which can be defined more generally by the proton donor–acceptor concept, is a driving force in the attainment of thermodynamic miscibility for many cases of polymer blends.

The blend system studied in this present paper is composed of a typical hydroxyl-containing polymer, poly(vinyl alcohol) (PVA), and a proton-accepting polymer, poly(*N*-vinyl pyrrolidone) (PVP), the latter with a carbonyl moiety in the side group. As was demonstrated in a previous publication[1], this polymer pair forms a miscible phase in the binary blends. Optically clear films were obtained by casting from mixed polymer solutions, and a single glass transition temperature (T_g) was situated between the T_gs of the two homopolymers for every blend composition. This good miscibility can be considered as being due to the capability of the two polymers to interact exothermally, which was supported by the evaluation of a negative polymer–polymer interaction parameter, i.e. $\chi_{12} = -0.35$ (at 513 K), from a thermodynamic melting point depression analysis. In fact, the presence of hydrogen bonding interactions between the carbonyl groups of PVP and the hydroxyl protons of PVA in this blend system was confirmed by Fourier transform infrared (*FT*i.r.) spectroscopy[2] and high-resolution solid-state ^{13}C n.m.r. techniques[3].

A noteworthy effect arising from the intimate mixing of PVA and PVP can be found in the optical properties of their oriented blends; the two polymers show intrinsic birefringences of opposite sign[1], as has been observed for several other miscible polymer pairs[4–6]. When a plain PVA film is stretched uniaxially, it exhibits a positive birefringence, i.e. $\Delta n = n_{\parallel} - n_{\perp} > 0$, where $n_{\parallel}$ is the refractive index parallel to the draw direction and $n_{\perp}$ is that measured perpendicular to it. In contrast, the other

*To whom correspondence should be addressed

0032-3861/94/07/1452–10

polymer (PVP), which has pyrrolidone rings attached to the main chain, shows negative birefringence. Accordingly, drawing of the binary blend films should give rise to certain characteristic changes in the optical anisotropy, which vary depending on the composition, as a result of the cooperative orientation development of the two interacting polymer components. This was exemplified in an earlier paper[1].

In this present paper, we provide further insight into the molecular orientation and optical anisotropy which are induced by stretching of PVA/PVP blends, in connection with the miscibility and interaction between the two components. A fluorescence polarization technique is employed to obtain information about the degree and type of molecular orientation, while birefringence is used as a measure for the estimation of the state of optical anisotropy of the drawn blends. A major discussion is given to the results obtained from the comparative experiments carried out for two series of samples, designated as PVA/PVP-H and PVA/PVP-L, where H and L indicate whether the molecular weight of the PVP is much higher (H) or lower (L) than that of PVA.

EXPERIMENTAL

Sample preparation

Atactic poly(vinyl alcohol) (PVA) was purchased from Polysciences, Inc.; the nominal molecular weight was 78 000 and the saponification value was 99.7 mol%. Two commercial samples of poly(*N*-vinyl pyrrolidone) (PVP), which differ in molecular weight, i.e. 350 000 (PVP-H) and 24 500 (PVP-L), were obtained from Nacalai Tesque, Inc. A water-soluble stilbene derivative, Whitex RP (Sumitomo Chemical Co.), was used as a probe for orientation estimation by a fluorescence polarization technique[7-12]. Its chemical structure is shown below:

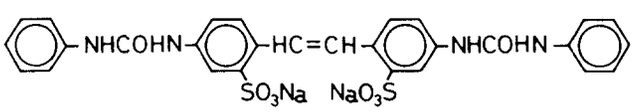

Dried powdered samples of PVA and PVP(-H or -L) were separately dissolved in distilled water at a concentration of 6.0 wt% (with continuous stirring), both at 70°C and at room temperature. A small amount of Whitex RP was dispersed into the two aqueous solutions at a concentration of 2.5×10^{-6} mol l^{-1}. The two solutions were mixed in the desired proportions and then stirred overnight at room temperature. The relative composition of the two polymers in the mixed solutions ranged from 10/90 to 90/10, expressed as ratios of weight percent, where the first number refers to the PVA content throughout this work. Both blend and homopolymer films of PVA and PVP were cast from aqueous solutions onto a Teflon plate by solvent evaporation at 45°C, and then dried further at ~50°C overnight, under vacuum. The concentration of fluorescent molecules in the cast films prepared in this way was $\sim 5 \times 10^{-5}$ mol l^{-1}, at which level any effect of fluorescence depolarization, caused by energy migration due to higher concentration of chromophores, is negligible[9,11].

Strips (5 × 30 mm in size), cut from the cast PVA/PVP films, were drawn uniaxially at 150–155°C, i.e. close to the T_g of PVP, in a silicone oil bath and then cooled quickly to ambient temperature (25°C). After washing with carbon tetrachloride, the drawn films were stored in a desiccator until needed. The draw ratio of the oriented samples was determined from the positions of marks on the films.

Measurements

Differential scanning calorimetry (d.s.c.) was conducted with a Seiko DSC-200 apparatus equipped with a thermal analysis station (SSC-5000). The measurements were carried out using 6–8 mg samples at a scanning rate of 20°C min^{-1} over the temperature range 10–250°C. The instrument was calibrated with an indium standard. The thermal data reported in this paper were recorded during the second scan, which gave stable d.s.c. traces for a series of the PVA/PVP blends.

The birefringence (Δn) of drawn PVA/PVP samples was determined by using an Olympus polarizing microscope equipped with a Berek compensator. The thickness of each film specimen was measured separately with a dial gauge.

Fluorescence polarization measurements were made by using an apparatus that had been built in our laboratory, which employed the optical system depicted in *Figure 1*, where the coordinate system O–*XYZ* is 'applied' to a drawn film so that the *Z*-axis is in the draw direction and the *Y*-axis is normal to the plane of the film surface. Light from a suitable source (a mercury arc lamp) was rendered parallel to the *Y*-axis by using a lens system. The light beam was then made monochromatic by means of a glass filter (Toshiba UV-D36B), which transmits a 365 nm mercury line, suitable for excitation

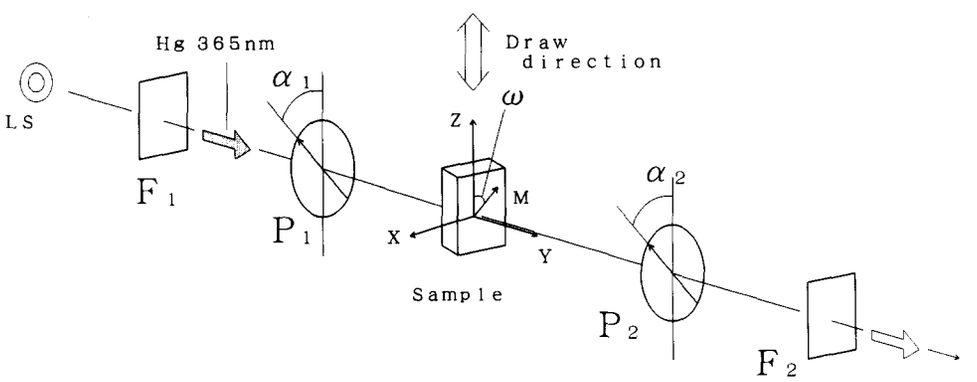

Figure 1 Schematic representation of the optical system used for measuring the polarized components of the fluorescence intensity: LS, mercury lamp (light source); F_1, monochromatic glass filter; P_1, polarizer; P_2, analyser; F_2, cut-off filter

of the Whitex RP fluorescent probe. The incident light was linearly polarized by a polarizer before reaching the sample. The fluorescence light emitted from the sample was detected by a phototube multiplier after passing through an analyser and a cut-off filter (SC-42, Fuji Photo Film Co.), employing a cut-off wavelength of 420 nm.

Four polarized components of the fluorescence intensity were measured by using the following combinations of the angles α_1 and α_2, which specify the alignments of the transmission axis of the polarizer ($\boldsymbol{P}_1$) and that of the analyser ($\boldsymbol{P}_2$), respectively: let I_{ZZ} be a polarized component of the fluorescence intensity which is observed when the axes $\boldsymbol{P}_1$ and $\boldsymbol{P}_2$ are both parallel to the Z-axis, i.e. $\alpha_1=\alpha_2=0°$, and I_{ZX} be a component obtained when $\boldsymbol{P}_1$ and $\boldsymbol{P}_2$ are parallel to the Z- and X- axes, respectively, i.e. $\alpha_1=0°$ and $\alpha_2=90°$. I_{XX} and I_{XZ} can be defined in a similar way. These components are not affected by a so-called birefringence effect[10,12] due to the optical anisotropy of the polymer medium, since the coordinate axes X, Y, and Z were chosen so as to coincide with the 'optically privileged' axes.

The orientation distribution of the molecular axis (M-axis) of the fluorescent probes was estimated in terms of the second and fourth moments, $\langle\cos^2\omega\rangle$ and $\langle\cos^4\omega\rangle$, respectively, which are defined by equation (1) in the next section. The quantities can be determined from equations (5)–(7) (see below) by using data for the polarized components of the fluorescence intensity, I_{ij} ($i,j=X$ or Z).

BACKGROUND AND PRELIMINARY CONSIDERATIONS

Fluorescence polarization and molecular orientation

In *Figure 2a*, the orientation of the molecular axis $\boldsymbol{M}$ of a fluorescent molecule is specified by a set of polar and azimuthal angles (ω,φ) in the sample coordinate system O-XYZ. The second and fourth moments of the molecular orientation about the Z-axis are defined in the following way:

$$\langle\cos^n\omega\rangle=\int_0^{2\pi}\int_0^{\pi}\cos^n\omega N(\omega,\varphi)\sin\omega\,d\omega\,d\varphi \quad (n=2,4) \tag{1}$$

where $N(\omega,\varphi)$ is a normalized function representing the molecular orientation distribution. The two moments can be combined with the observed quantities, i.e. the polarized components of the fluorescence intensity, as shown below.

The selective light absorption of fluorescent molecules and the polarization characteristics of the emitted fluorescence are, in general, explicable in terms of an oscillator model (see *Figure 2b*): when a fluorescent molecule having an absorbing oscillator $\boldsymbol{A}$ is excited by polarized light with an electric vector $\boldsymbol{E}_i$, the probability of excitation, i_a, is proportional to the square of a scalar product of $\boldsymbol{E}_i$ and $\boldsymbol{A}$, i.e.

$$i_a=k(\boldsymbol{E}_i\boldsymbol{A})^2 \tag{2}$$

Subsequently, if the fluorescence light emitted from an oscillator $\boldsymbol{F}$ of the excited molecule is detected as a component with its vibration axis $\boldsymbol{E}_j$, the probability of detection, i_f, is represented as

$$i_f=\phi(\boldsymbol{F}\boldsymbol{E}_j)^2 \tag{3}$$

In photostationary measurements, the overall intensity (I_{ij}) of the polarized component of the fluorescence obtained from the system can be written in the following fashion:

$$I_{ij}=k\phi\int_0^{2\pi}\int_0^{\pi}N(\omega,\varphi)\overline{(\boldsymbol{E}_i\boldsymbol{A})^2}\,\overline{(\boldsymbol{F}\boldsymbol{E}_j)^2}\sin\omega\,d\omega\,d\varphi \tag{4}$$

In this formulation, some potential distribution of the oscillators $\boldsymbol{A}$ and $\boldsymbol{F}$ around the molecular axis $\boldsymbol{M}$ is also taken into account, i.e. the excitation and detection probabilities are averaged with respect to a pair of angles (δ,ε) and (η,ξ), respectively, which specify the orientation of the absorbing and emitting oscillators in the molecular framework O-KLM, as shown in *Figure 2b*.

In the optical arrangement where the electric vectors $\boldsymbol{E}_i$ and $\boldsymbol{E}_j$ are parallel to the X- or Z-axis of the polymer sample, the polarized component of the fluorescence intensity I_{ij} ($i,j=X$ or Z) can be calculated as follows:

$$I_{ZZ}=(k\phi/9)[1+(a_0+f_0)W_1+a_0f_0W_2] \tag{5a}$$

$$I_{ZX}=(k\phi/9)[1+(1/2)(2a_0-f_0)W_1-(1/2)a_0f_0W_2] \tag{5b}$$

$$I_{XX}=(k\phi/9)[1-(1/2)(a_0+f_0)W_1+(1/4)a_0f_0W_2+(9/8)a_0f_0W_3] \tag{5c}$$

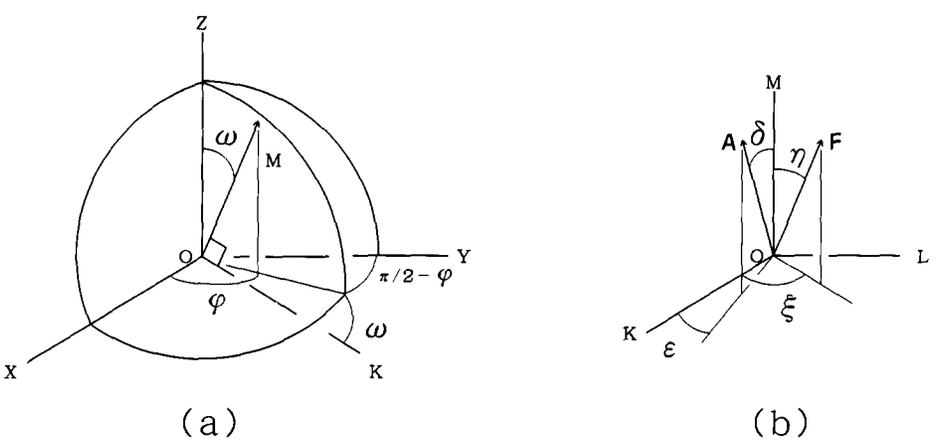

Figure 2 Angular specifications for the orientation axes: (a) molecular axis $\boldsymbol{M}$ of a fluorescent probe, oriented at the polar and azimuthal angles, ω and φ, respectively, in a O-XYZ coordinate system fixed to a polymer sample; (b) absorbing ($\boldsymbol{A}$) and emitting ($\boldsymbol{F}$) oscillators lying along the directions of (δ,ε) and (η,ξ), respectively, within the O-KLM molecular framework

$$I_{XZ}=(k\phi/9)[1+(1/2)(2f_0-a_0)W_1-(1/2)a_0f_0W_2] \quad (5d)$$

where

$$W_1=3\langle\cos^2\omega\rangle-1 \quad (6a)$$

$$W_2=9\langle\cos^4\omega\rangle-6\langle\cos^2\omega\rangle+1 \quad (6b)$$

$$W_3=\langle\cos^4\omega\rangle-2\langle\cos^2\omega\rangle+1 \quad (6c)$$

and

$$a_0=(3\overline{\cos^2\delta}-1)/2 \quad (7a)$$

$$f_0=(3\overline{\cos^2\eta}-1)/2 \quad (7b)$$

Equations (7a) and (7b) indicate that a_0 and f_0 are parameters that characterize the intrinsic photophysical anisotropy of the fluorescent molecule which is used as an orientation probe. For the stilbene derivative Whitex RP, the anisotropy of light absorption and that of emission were found to be similar in extent, i.e., $a_0\approx f_0$, since the observed intensities I_{ZX} and I_{XZ} were almost equal to each other, irrespective of the degree of orientation of the drawn samples. In the present study, a value of $a_0\approx f_0=0.91$ was adopted, which was evaluated from the following relationship applicable to undrawn samples with a random orientation distribution:

$$(I_{ZZ}-I_{ZX})/(I_{ZZ}+2I_{ZX})=(2/5)a_0f_0 \quad (8)$$

Relationship between birefringence and orientation functions

Optical birefringence derives from the orientation of polymer chains which have inherently the anisotropy of the polarizability. In the simplest case of uniaxial stretching of amorphous homopolymers, the extent of birefringence Δn varies monotonically with the degree of orientation, irrespective of whether Δn is positive or negative, according to the following equation:

$$\Delta n=(1/2)(3\langle\cos^2\omega_s\rangle-1)\Delta n^\circ \quad (9)$$

where Δn° is a limiting birefringence for the perfect uniaxial orientation of polymer chains, and $\langle\cos^2\omega_s\rangle$ is the second moment of orientation for an anisotropic unit $\boldsymbol{S}$ with a certain polarizability. In the birefringence method, however, it is not so easy to precisely stipulate the size of the orientation unit $\boldsymbol{S}$; here, for convenience, we let the unit be a statistical chain segment which is less than several angstroms in length.

On the other hand, the structural unit for orientation measurement by the fluorescence method is a rod-like probe ($\boldsymbol{M}$) of a definite molecular size, which is incorporated into the amorphous regions of the polymer material; for example, its length is $\sim$2.5 nm in the case of Whitex RP. The illustrations given in *Figure 3* clarify the differences in size and orientation angle between the two structural units $\boldsymbol{S}$ and $\boldsymbol{M}$ as defined above. As shown on the left side of the figure, the vectors $\boldsymbol{S}$ and $\boldsymbol{M}$ are oriented at angles ω_s and ω, respectively, to the Z-axis, while the orientation of $\boldsymbol{S}$ to the $\boldsymbol{M}$-axis is specified by θ and χ. Using a theorem taken from spherical trigonometry, the following relationship holds among all of these angles:

$$\cos\omega_s=\cos\omega\cos\theta+\sin\omega\sin\theta\cos\chi \quad (10)$$

Assuming the distribution of $\boldsymbol{S}$ around the $\boldsymbol{M}$-axis to be rotationally symmetrical, i.e. to be independent of χ, we can derive the following expression from equation (10):

$$(3\langle\cos^2\omega_s\rangle-1)/2=[(3\langle\cos^2\theta\rangle-1)/2]\times[(3\langle\cos^2\omega\rangle-1)/2] \quad (11)$$

which expresses a relationship among the following three orientation functions:

$$f_s=(3\langle\cos^2\omega_s\rangle-1)/2 \quad (12a)$$

$$f=(3\langle\cos^2\omega\rangle-1)/2 \quad (12b)$$

$$f'=(3\langle\cos^2\theta\rangle-1)/2 \quad (12c)$$

Accordingly, equation (9) can be rewritten, by using equations (11) and (12), as follows:

$$\Delta n=f_s\Delta n^\circ=f'f\Delta n^\circ \quad (13)$$

In the case of the stretching of a blend composed of polymer 1 and polymer 2, Δn of the deformed sample may be represented by

$$\Delta n=v_1\Delta n_1+v_2\Delta n_2 \quad (14)$$

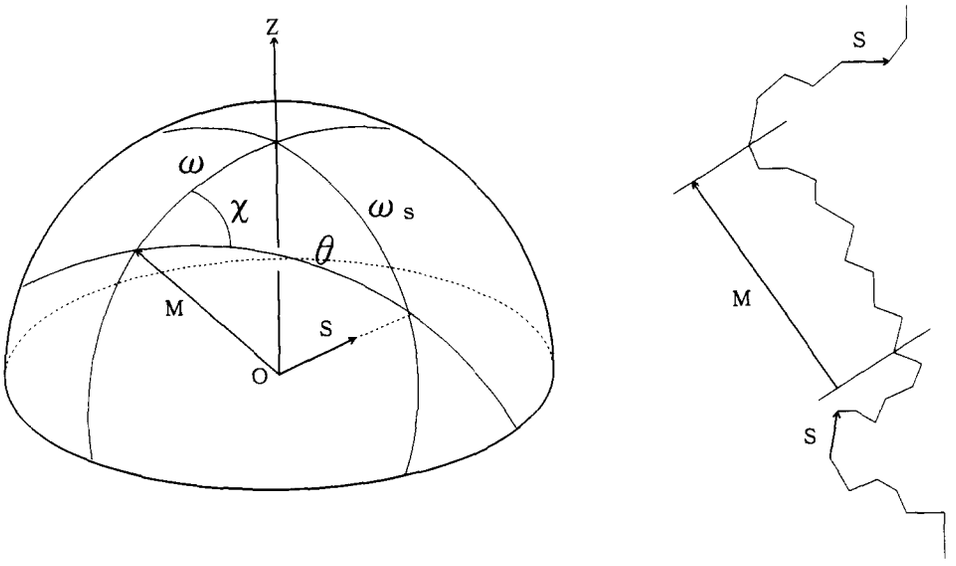

Figure 3 Schematic representations of two structural units $\boldsymbol{M}$ and $\boldsymbol{S}$ oriented at different angles to the stretching axis Z: $\boldsymbol{M}$ is the molecular axis of a fluorescent probe with a length of $\sim$2.5 nm, and $\boldsymbol{S}$ is a statistical segment, of shorter length, having a specific anisotropy in polarizability

where $v_i\Delta n_i$ $(i=1,2)$ indicates the contribution of an oriented polymer component i to the total birefringence and v_i denotes the volume fraction of that component. If the sample contains a crystalline phase of a component i, Δn_i should be divided into two terms, taking account of the degree of crystallinity. In the following treatment, the polymer blend, for convenience, is considered to be an overall amorphous material which exhibits a high level of miscibility.

Let us consider the case where the upper scale limit in heterogeneity of the polymer–polymer mixing is comparable to the length of the fluorescent probe used, ~2.5 nm in this present study. This is quite a reasonable assumption for the PVA/PVP system, as a mixing scale of 2–3 nm has been determined for the miscible phase in a recent study by solid-state n.m.r. spectroscopic techniques[3]. On stretching films of such a blend, ideally the two component polymers would be oriented equally at the miscibility level, and their orientation behaviour may be characterized in terms of a common function f, referring to an orientation probe of the same size as the mixing scale. On a few angstroms scale, however, it may be plausible that different kinds of chain segments behave rather differently. Therefore, equation (14) can be re-written as follows, by using the relationship (13) for Δn_i of each component:

$$\Delta n = v_1 f_{s1}\Delta n_1^\circ + v_2 f_{s2}\Delta n_2^\circ$$
$$= (v_1 f_1'\Delta n_1^\circ + v_2 f_2'\Delta n_2^\circ) f \qquad (15)$$

where f_{si} and f_i' refer to the segmental orientation functions for the component i.

Birefringence compensation

In the PVA/PVP system, the two constituent polymers show intrinsic birefringences of opposite sign, i.e.

$$\Delta n_1^\circ < 0 \quad \text{and} \quad \Delta n_2^\circ > 0$$

where the subscripts, 1 and 2, are used to designate the PVP and PVA components, respectively. Therefore, there should be some compensation between the positive and the negative contributions to the total birefringence in the drawn blends. Of particular interest in this present paper is the dependence of the overall birefringence on the molecular weight of the PVP component. Let us make a comparison here between the two series of blends, PVA/PVP-H and PVA/PVP-L, which have been deformed under the same conditions.

In the drawing process, the PVP-H molecules of longer chain length (and therefore longer relaxation times), when compared to the PVP-L molecules, have a greater advantage in the attainment of a higher degree of segment orientation. In addition, it may be expected that the higher the molecular weight of PVP, the higher will be the frequency of occurrence of the carbonyl–hydroxyl interactions between PVP and PVA, at least for the PVP chain, resulting in a more effective restraint of the orientation relaxation of the PVP segments. A recent *FT*i.r. study[2] supports this assumption of a chemical interaction effect. Therefore, appreciable differences will occur in the magnitude of the functions f_{s1} and f_1' with respect to the orientation of the PVP segments, between the two series of blends, i.e.

$$f_{s1}(\text{PVP-H}) > f_{s1}(\text{PVP-L})$$
$$f_1'(\text{PVP-H}) > f_1'(\text{PVP-L})$$

Within the scope of the above considerations, we deduce the following predictions, using equation (15):

(i) A composition range where PVA/PVP drawn blends show negative optical anisotropy, will be much wider in the PVA/PVP-H series than in the case of the PVA/PVP-L series, i.e. a critical PVP concentration, v_{1c}, above which drawn samples show a negative value of Δn, will be much lower in the PVA/PVP-H series.

(ii) PVA/PVP-H drawn blends will give a smaller Δn value, compared with PVA/PVP-L blends of the same composition, even if both series of samples are elongated to give an equal degree of orientation (f) in a structural unit of ~2.5 nm scale.

RESULTS AND DISCUSSION

The results of d.s.c. measurements carried out on a number of PVA/PVP-H samples are shown in *Figure 4*. For all of the compositions investigated, a single glass transition is detected, with the temperature (T_g) varying with composition between the T_g values of the two component polymers. It is therefore considered that the

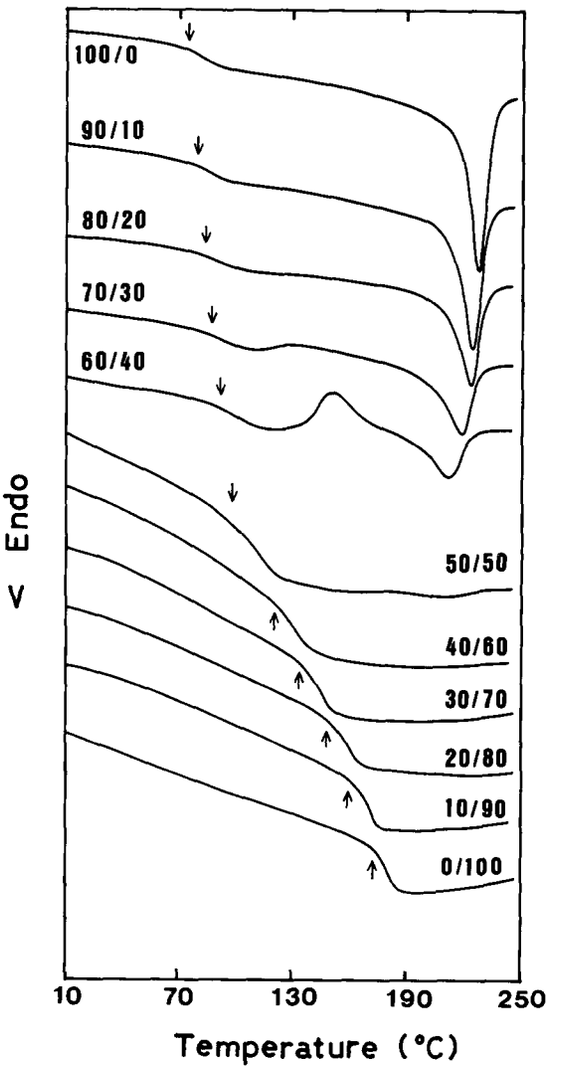

Figure 4 D.s.c. thermograms for a series of PVA/PVP-H samples; the sensitivity of the scans for the samples of composition 50/50–0/100 is about three times that of the others. Arrows indicate a T_g position which is taken as the onset point of the discontinuity in heat flow

polymer pair is miscible, at least in the non-crystalline fraction of the mixture. A melting peak of PVA, with its maximum originally at 229°C, systematically shifts to lower temperatures as PVP is blended (up to a content of 40 wt%); at a 50/50 composition it barely becomes discernible in the d.s.c. curve. An endothermic peak appearing in the d.s.c. data for a PVA/PVP (60/40) sample is due to the fusion of PVA crystals that takes place during the heating scan; a cold-crystallization phenomenon takes place after the glass transition of the blend on heating, with the resulting exothermic peak being of almost the same area as that of the melting peak. Such effects of a depression in the melting point and a repression in the development of crystallinity of the crystallizable component (i.e. PVA), due to addition of the second component (PVP), are common features which are shared with other crystalline/amorphous polymer pairs that are capable of forming a miscible phase in their blends[13–16].

The thermal transition behaviour of a series of PVA/PVP-L samples has already been described in detail in a previous paper[1]. Comparing these present results for the PVA/PVP-H series with those obtained for the PVA/PVP-L series (see Figures 3 and 6 in ref. 1), we find that the former blends give rather higher T_gs especially for compositions which are rich in PVP, i.e. by ~10–25°C for PVA/PVP (40/60–0/100) compositions. In addition, the PVP concentration at which the crystal fusion of PVA no longer becomes observable is lower in the case of the PVA/PVP-H blends, i.e. ΔH_f is essentially zero at PVP concentrations $\geqslant$50 wt% for PVA/PVP-H and $\geqslant$70 wt% for PVA/PVP-L, where ΔH_f is an apparent enthalpy of fusion, which is proportional to the area of a melting peak. This is in accordance with results obtained from *FT*i.r. measurements[2], i.e. the higher the molecular weight of the PVP, the more effective is the hindrance to PVA crystallization.

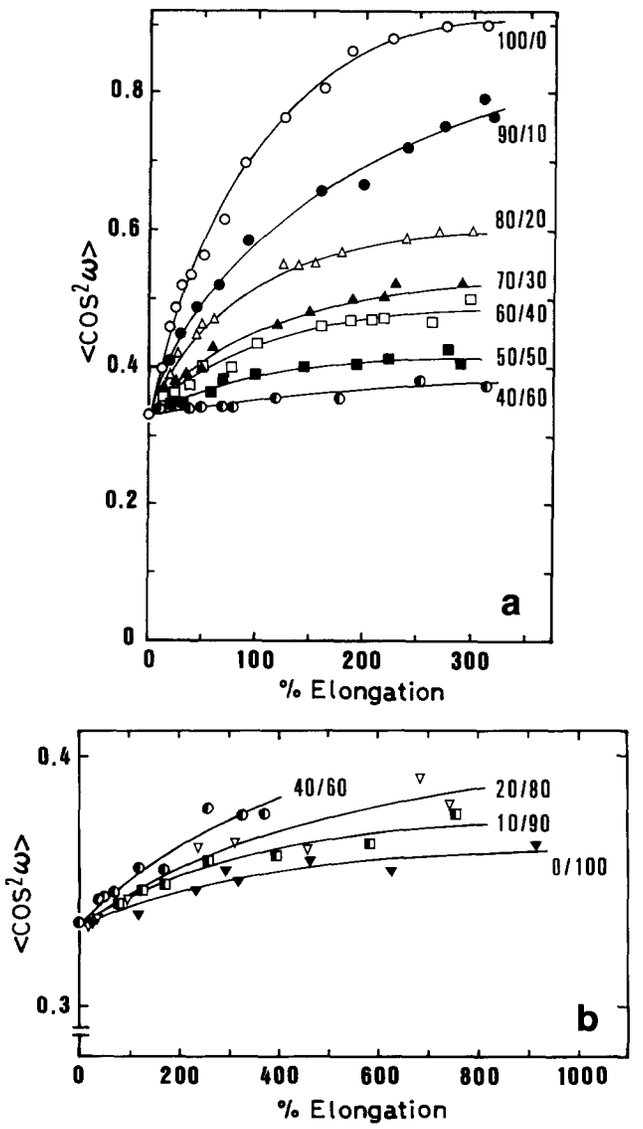

Figure 5 Plots of $\langle\cos^2\omega\rangle$ *versus* % elongation for PVA/PVP-L blends, with PVP-L contents: (a) 0–60 wt%; (b) 60–100 wt%

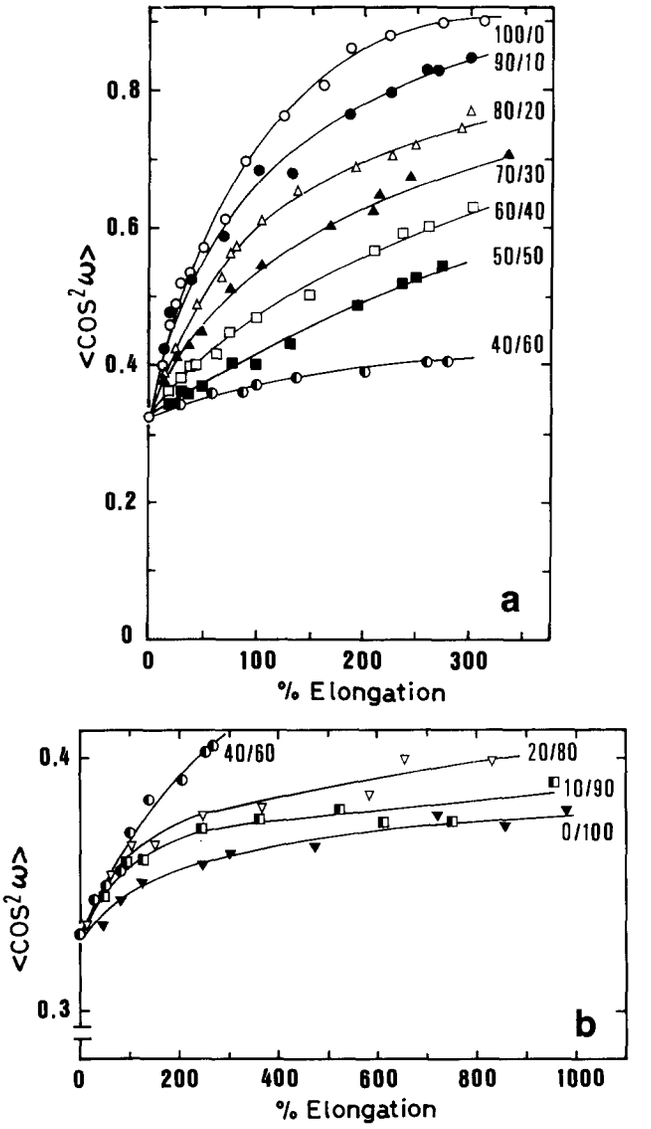

Figure 6 Plots of $\langle\cos^2\omega\rangle$ *versus* % elongation for PVA/PVP-H blends, with PVP-H contents: (a) 0–60 wt%; (b) 60–100 wt%

In *Figures 5* and *6*, the second moment of molecular orientation, $\langle\cos^2\omega\rangle$, evaluated by the fluorescence polarization method, is plotted against the percentage elongation of film specimens of PVA/PVP-L and PVA/PVP-H blends, respectively. In both series of blends, the value of $\langle\cos^2\omega\rangle$ increases monotonically from 0.333 with increasing extent of elongation, irrespective of the composition. As is well known[9,10,17,18] PVA homopolymer films show quite a high level of molecular

orientation on stretching. The capability of this polymer for high degrees of orientation may be attributed to the strong hydrogen-bonding interactions between the hydroxyl groups. In contrast, a considerably lower level of orientation prevails in drawn PVP films even after extremely large deformations; the specimens were, actually, highly susceptible to plastic flow during deformation at the drawing temperature of ~150°C. It should be stressed, however, that the drawn films give a decidedly 'positive' orientation function, i.e. $f=(3\langle\cos^2\omega\rangle-1)/2>0$, indicating a normal trend for molecular orientation in the draw direction.

If we consider the blends of PVA and PVP(-L or -H), the $\langle\cos^2\omega\rangle$ *versus* percentage elongation plots are always located between the corresponding plots obtained for the two homopolymers. The degree of orientation decreases monotonically with an increase in PVP content, when compared at a given stage of elongation. According to the *FT*i.r. data presented by Ping *et al.*[2] on the blending of PVA with PVP of a less self-associating nature, more and more of the hydroxyl–hydroxyl bonds in PVA are broken as the PVP content is increased. Concomitantly, some of the hydroxyl protons liberated from interactions with the oxygen atoms of other hydroxyl groups, in turn, become involved in hydrogen bonding with the carbonyl oxygens of PVP, which has inherently less capability for orientation. In view of this convincing argument, it is conceivable that the two polymers must have been oriented, considerably cooperatively, in the miscible amorphous regions of the blend films during the course of the uniaxial stretching process.

Comparing the molecular orientation behaviour shown in *Figures 5* and *6* between the two series of blends at equivalent PVA/PVP proportions, it is found that the PVA/PVP-H samples exhibit a higher degree of orientation than the PVA/PVP-L samples. One can readily understand this observation, since the molecular mobility and orientation relaxation are more limited in a more viscous medium which contains a polymer species with a higher molecular weight. In addition to this primary feature, the higher the molecular weight of PVP, the greater is the number of carbonyl groups associated with hydrogen bondings with the PVA hydroxyls, as is again confirmed by the *FT*i.r. results[2]. Therefore, at a given PVP content the PVA/PVP-H blend could be considered as a more dense, 'quasi-network system', when compared to the corresponding PVA/PVP-L blend. A higher density of cross-links is also in favour of a restriction of the possible relaxation of the molecular orientation in the deformed polymer network.

Using the fluorescence polarization technique, it is possible to obtain information about not only the degree, but also the type of molecular orientation in the non-crystalline regions of polymeric solids[7–12]. A convenient method for estimating the type of molecular orientation is to construct a plot of the fourth moment against the second moment of orientation and to then search for conformity of the plot to a relationship between the moments calculated in terms of some potential model of the orientation distribution. Various examples of construction of the $\langle\cos^4\omega\rangle$ *versus* $\langle\cos^2\omega\rangle$ plot are shown in *Figure 7* for selected blends of PVA with PVP-L (*Figure 7a*) and PVP-H (*Figure 7b*), with the films being deformed to a draw ratio (λ) of 3.1–3.5. The continuous lines in the respective figures represent a relationship derived by assuming that the molecular orientation

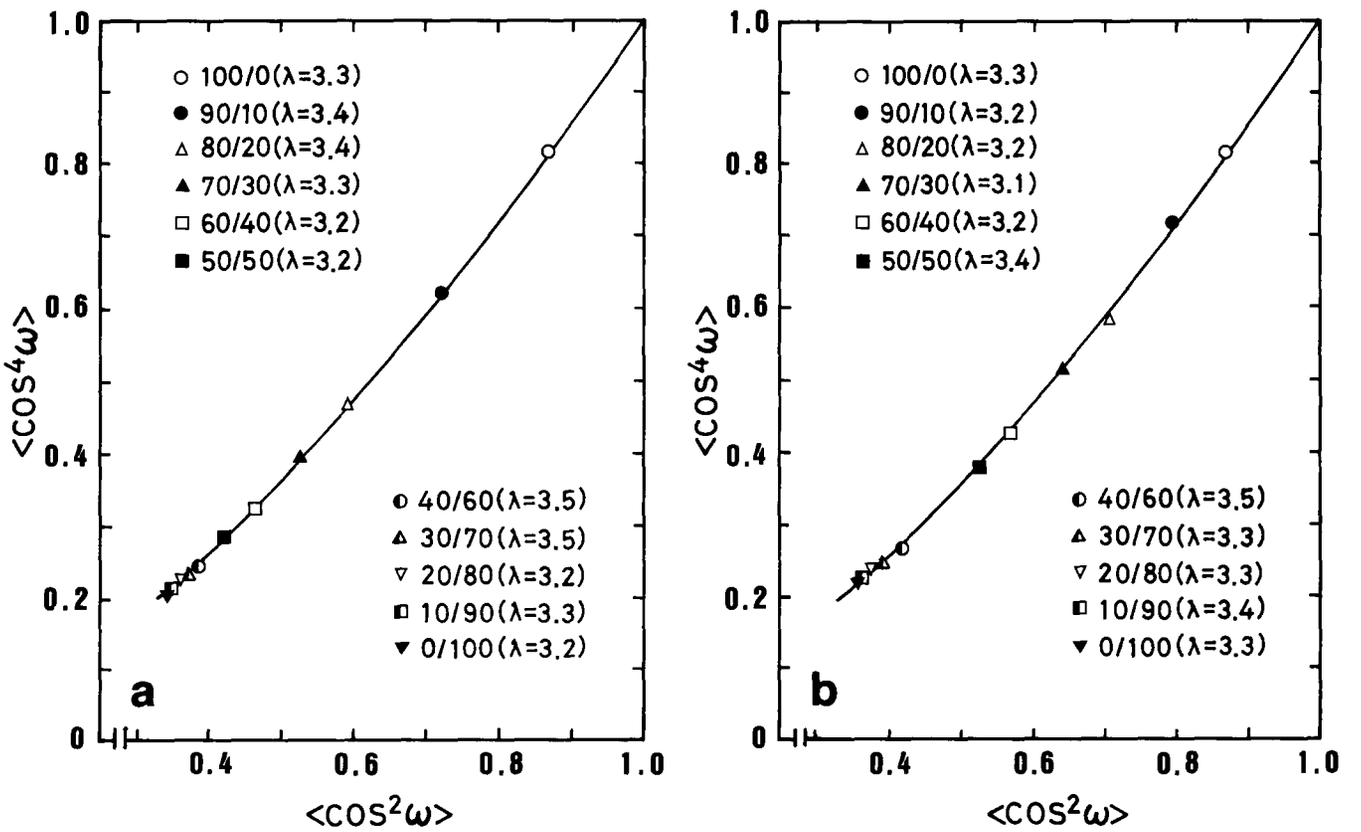

Figure 7 Plots of $\langle\cos^4\omega\rangle$ *versus* $\langle\cos^2\omega\rangle$ for (a) PVA/PVP-L and (b) PVA/PVP-H samples deformed uniaxially to a draw ratio (λ) of 3.1–3.5. The continuous lines represent a relationship between the two moments calculated in terms of a model of a prolate ellipsoid of rotation for the type of molecular orientation distribution

distribution obeys a type of prolate ellipsoid of rotation about the stretching axis. The calculated curve is virtually equivalent to a theoretical curve predicted by a Kratky-type affine deformation scheme[19], proposed for the orientation of rods floating in a bulk matrix. In the case of uniaxial stretching of PVA homopolymer films containing Whitex RP, it is already known[9,10,12] that the type of orientation distribution of the fluorescent molecules fits this model satisfactorily.

When PVP is incorporated with PVA, as has already been revealed in *Figures 5* and *6*, the molecular orientation development in the drawn blends is somewhat delayed, when compared with the rapid transformation observed for 'pure' PVA on stretching. Corresponding to this behaviour, the position of the data points in the $\langle\cos^4\omega\rangle$ *versus* $\langle\cos^2\omega\rangle$ plots in *Figures 7a* and *7b* shift progressively toward the lower and left side with increasing PVP content, with the blending effect being usually more prominent in the PVA/PVP-L series. However, the experimental data for all of the compositions lie on the calculated curve. In such an application of the combined use of the second and fourth moments, it was confirmed that the type of molecular orientation distribution in the uniaxially deformed PVA/PVP blends followed well the model of a prolate ellipsoid of rotation

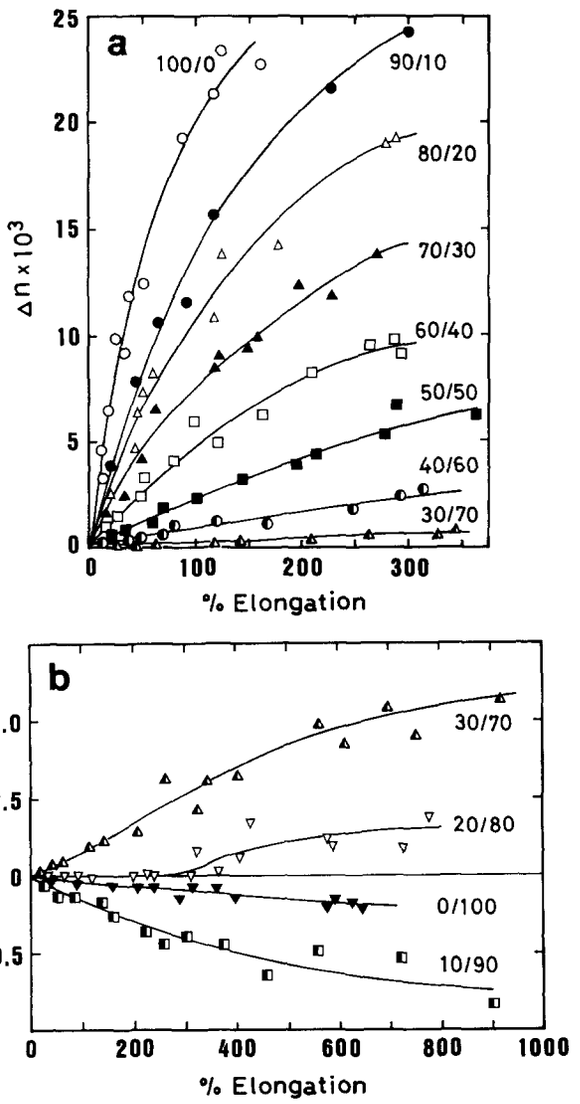

Figure 8 Birefringence *versus* % elongation for drawn PVA/PVP-L blends, with PVP-L contents: (a) 0–70 wt%; (b) 70–100 wt%

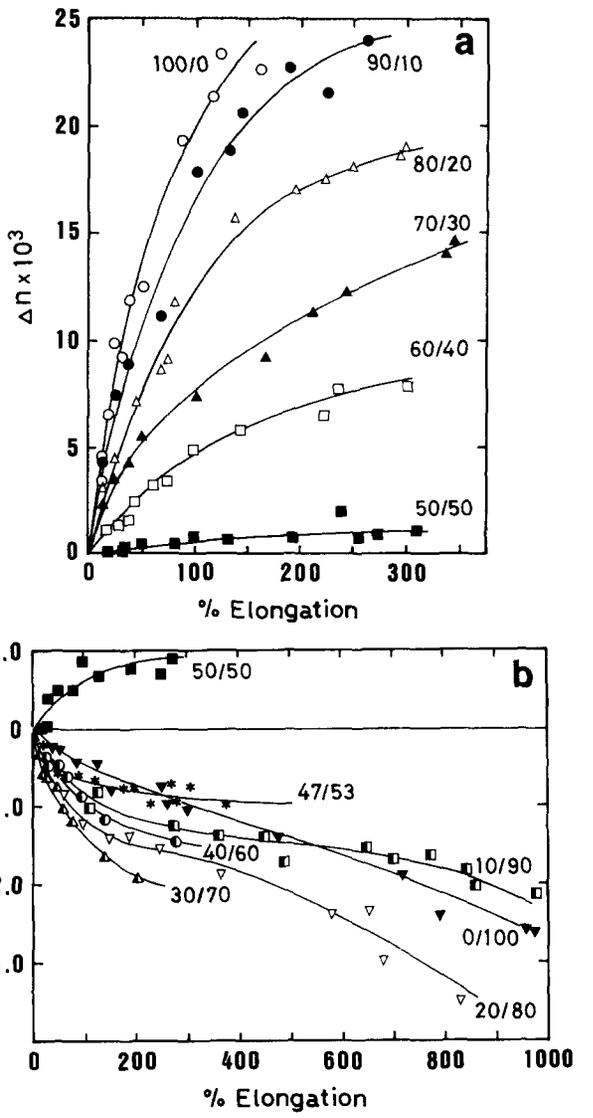

Figure 9 Birefringence *versus* % elongation for drawn PVA/PVP-H blends, with PVP-H contents: (a) 0–50 wt%; (b) 50–100 wt%

at every stage of elongation, irrespective of the composition or the PVP molecular weight.

Figures 8 and *9* show the results of the birefringence measurements carried out on drawn PVA/PVP-L and PVA/PVP-H films, respectively. Plots of Δn *versus* percentage elongation are constructed for a wide range of compositions of the respective series of blends. As demonstrated in *Figures 8a* and *9a*, PVA homopolymer exhibits positive optical anisotropy ($\Delta n > 0$) on stretching; the value of Δn shows a remarkable increase with increasing elongation. On the other hand, drawn PVP films show a definitely negative birefringence, as seen in *Figures 8b* and *9b*, notwithstanding the fact that the induced optical anisotropy is relatively low, particularly in the PVP-L samples. The small magnitude of Δn observed for the PVP samples can be attributed primarily to the prevalence of a lower degree of orientation of the polymer molecules in the stretched samples.

Of particular interest is the dramatic change in the Δn *versus* percentage elongation plot with composition. The ways in which the changes occur in the two series of blends are rather different from each other and also distinct from the monotonic suppression in the rise of the $\langle\cos^2\omega\rangle$ *versus* percentage elongation curves with an increasing PVP content. The following observations

concerning the birefringence data are worth noting, in comparisons between the two series of PVA/PVP blends:

(1) In the composition range of 100/0–60/40, there is less difference in the location of the Δn *versus* percentage elongation curves between the two series; however, caution should be given to the fact that the PVA/PVP-H blends exhibited a higher degree of molecular orientation than the PVA/PVP-L blends at every stage of elongation. With the PVA-rich compositions, PVA crystallinity persists in the blends (see *Figure 4*), and hence it should also be noted that the orientation of the PVA crystals makes a positive contribution to the total birefringence of the drawn samples, and to an appreciable extent. At compositions containing $\geqslant 50$ wt% PVP, the PVA/PVP-H series, which is capable of higher orientation, gives decidedly much lower Δn values than the other series.

(2) A minimal PVP fraction, w_{1c}, above which the drawn blends show negative birefringence, is much smaller in the PVA/PVP-H series ($0.5 < w_{1c} < 0.53$) than in the case of the PVA/PVP-L system, where w_{1c} appears to have a value which is slightly larger than 0.8.

(3) At PVP-rich concentrations above w_{1c}, drawn blends tend to show more negative birefringence than drawn, pure PVP; this is observed as a common feature in both series.

In the present oriented system, there evidently exists a compensation effect due to the positive and negative contributions of the PVA and PVP, respectively, to the overall birefringence. Observations (1) and (2) presented above indicate that the negative contribution of PVP is more intensely pronounced in the drawn blends containing higher-molecular-weight PVP. Observation (2) is in fact consistent with a prediction deduced in a preliminary consideration of the molecular weight dependence of the birefringence compensation effect, i.e. the higher the molecular weight of PVP, the wider is the composition range where drawn PVA/PVP blends show a negative birefringence.

From observation (3), it can be said that orientation of the PVP molecules is appreciably enhanced in the presence of PVA, possibly by virtue of the interpolymer interactions that occur through hydrogen bonding between the hydroxyl and carbonyl groups. This observation is also one of the pieces of evidence for good miscibility in the present system. In interpreting the cooperative behaviour of the two components, however, caution should be exercised regarding the following point: it is most likely that the PVA and PVP molecules are oriented in a still different way at the segmental level in the drawn blends, in spite of the indication of considerable miscibility. If the segmental orientations of both components were identical to each other, i.e. a relationship of the $f_{s1} = f_{s2}$ holds for the orientation functions defined previously, there would be a determinate composition which is characteristic of the polymer pair being considered, at which the blend remains a birefringence-free material, no matter how much molecular orientation is induced. This is because, according to equation (15), such a composition is given uniquely by a ratio of the intrinsic birefringences of the two polymer species, on the assumption that $\Delta n = 0$ while $f_{s1} = f_{s2} > 0$. However, as

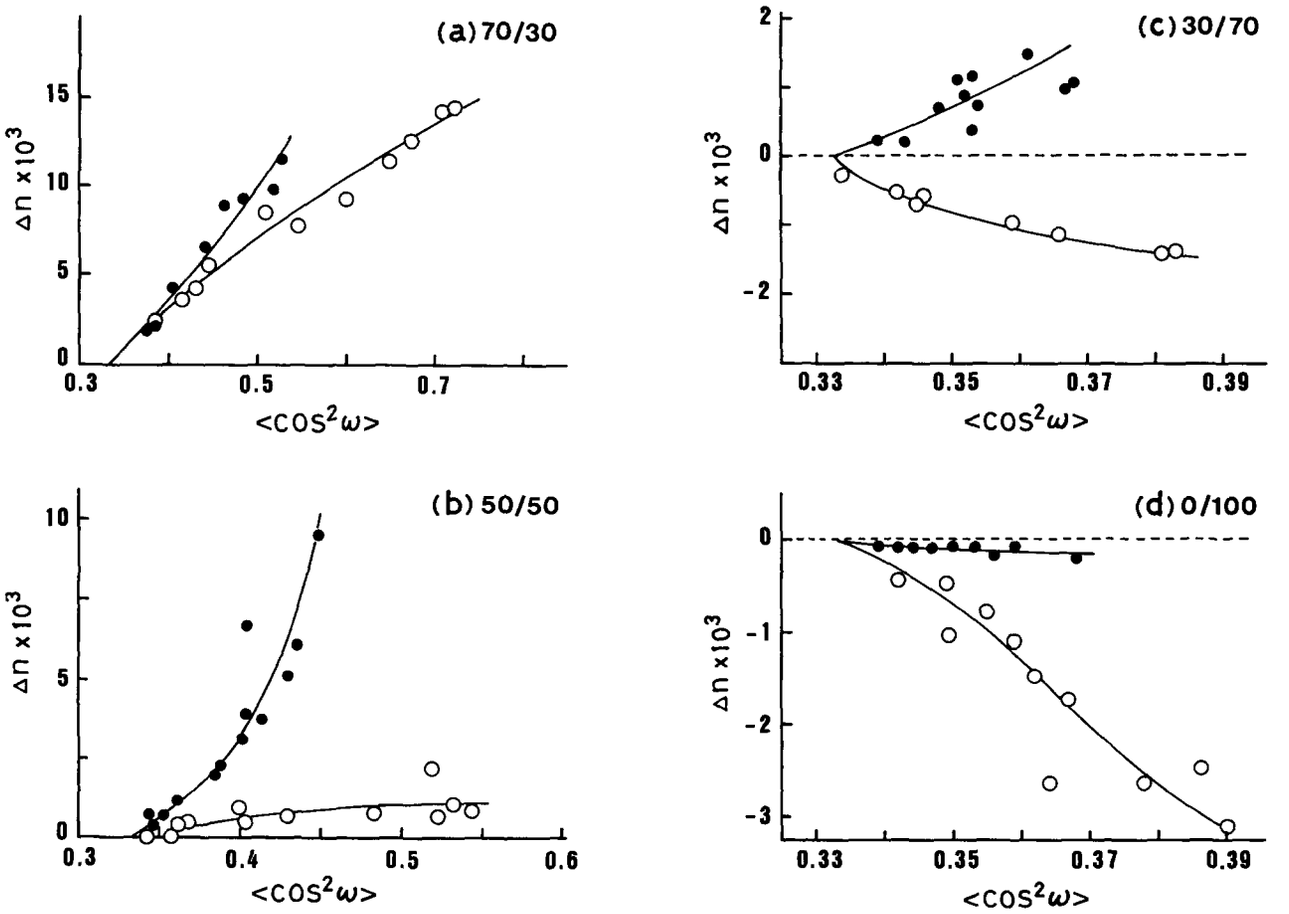

Figure 10 Birefringence *versus* $\langle \cos^2 \omega \rangle$ for selected compositions of PVA/PVP-L (●) and PVA/PVP-H (○): (a) 70/30; (b) 50/50; (c) 30/70; (d) 0/100

stated in observation (2), we found too large a difference in the critical PVP concentration (w_{1c}) between the two series of blends, with both being a thermodynamically miscible system composed of the same pairs of polymer species. An ideal way to evaluate this critical concentration is to specify the composition which gives rise to zero-birefringence, irrespective of the draw ratio of the blend or the degree of molecular orientation which is induced. In view of this fact, it is reasonable to assume that the chain segments of the two polymer components orient differently when subjected to uniaxial extension, despite the compatible nature of the blends. This is the same conclusion as the one drawn by Monnerie and co-workers[6,20-22] for the orientation behaviour of a range of blends composed of various miscible polymer pairs.

In *Figure 10*, Δn values are plotted as a function of the second moment of orientation for selected compositions of the two series of PVA/PVP blends. As is evident from the plots, even though PVA/PVP-H and PVA/PVP-L samples of the same composition are oriented to an equal degree when viewed in a structural unit with an approximate 2.5 nm scale, the former shows a smaller birefringence than the latter. At a PVA-rich composition of 70/30 (see *Figure 10a*), there appears to be a relatively small difference in the Δn *versus* $\langle\cos^2\omega\rangle$ data between the two series. A large, positive contribution of the birefringence arising from the orientation of the remaining PVA crystals to the total birefringence may be responsible for this apparent small difference.

The above result also clearly demonstrates that PVP-H acquires a higher 'segmental' orientation and hence makes, more effectively, a negative contribution to the birefringence, than does the same concentration of PVP-L. This is explicable in terms of the molecular weight dependence of the extent of relaxation of the PVP chains which occurs during the experimental stretching process, as discussed in the preceding text.

SUMMARY AND CONCLUSIONS

Poly(vinyl alcohol)/poly(*N*-vinyl pyrrolidone) (PVA/PVP) is a thermodynamically miscible pair, as evidenced by d.s.c. analysis: the blends exhibit a composition-dependent, single T_g which is situated between the T_gs of the individual components. A comparative study of the molecular orientation and optical anisotropy induced by uniaxial stretching of the PVA/PVP films was undertaken for two series of samples with different PVP components, with molecular weights which were either much higher (PVP-H) or lower (PVP-L) than the PVA component. An estimation of molecular orientation was carried out by using the second ($\langle\cos^2\omega\rangle$) and fourth ($\langle\cos^4\omega\rangle$) moments, obtained by the use of the fluorescence polarization method. The stilbene derivative molecule, Whitex RP, with an approximate 2.5 nm length, was utilized as a probe for the orientation measurements.

Both series of PVA/PVP blends imparted a positive orientation function, i.e. $f=(3\langle\cos^2\omega\rangle-1)/2>0$, on stretching, irrespective of the composition. The form of the molecular orientation distribution agreed well with the prolate ellipsoid model of uniaxial rotation. The degree of molecular orientation decreased monotonically with an increasing PVP content in the blends, when compared at the same extent of elongation over the wide range of compositions investigated. PVA/PVP-H drawn blends acquired a higher degree of orientation than the PVA/PVP-L drawn blends with corresponding compositions.

The two component polymers showed a mutually opposite sign in the intrinsic birefringence, and the drawing of the blend films gave rise to a characteristic change in the optical anisotropy with composition. The extent of birefringence (Δn) of the drawn films, when compared at a given draw ratio for a series of blends, decreased rapidly with an increase in the PVP fraction (w_1) until w_1 reached a certain value (w_{1c}) at which Δn changed from positive to negative. At PVP-rich concentrations above w_{1c}, the negative birefringence observed for the drawn blends was generally greater in absolute value than that of the drawn, pure PVP. This implies that the two constituent polymers can orient cooperatively to a considerable extent as a result of their miscibility. The critical PVP fraction w_{1c} was much smaller in the PVA/PVP-H series ($0.5<w_{1c}<0.53$) than in the case of the PVA/PVP-L series ($0.8\lesssim w_{1c}<0.9$). Therefore, the higher the molecular weight of PVP, the wider is the composition range over which drawn PVA/PVP blends show negative optical anisotropy. Even if both series of blends were deformed to give an equal degree of orientation when viewed in the fluorescent probe unit of 2.5 nm, PVA/PVP-H drawn films exhibited a smaller birefringence than the corresponding PVA/PVP-L samples. In the deformation process, the segmental relaxation of PVP-H molecules with longer chain lengths is possibly more restricted than in the case with shorter lengths, by virtue of the higher frequency of specific interactions with the PVA molecules. This results in more prominence of the negative contribution of oriented PVP to the overall birefringence in the series of drawn blends with PVP-H rather than with PVP-L.

REFERENCES

1 Nishio, Y., Haratani, T. and Takahashi, T. *J. Polym. Sci. Polym. Phys. Edn* 1990, **28**, 355
2 Ping, Z. H., Nguyen, Q. T. and Néel, J. *Makromol. Chem.* 1990, **191**, 185
3 Zhang, X., Takegoshi, K. and Hikichi, K. *Polymer* 1992, **33**, 712
4 Hahn, B. R. and Wendorff, J. H. *Polymer* 1985, **26**, 1619
5 Saito, H. and Inoue, T. *J. Polym. Sci. Polym. Phys. Edn* 1987, **25**, 1629
6 Zhao, Y., Jasse, B. and Monnerie, L. *Polymer* 1991, **32**, 209
7 Nishijima, Y. *J. Polym. Sci. (C)* 1970, **31**, 353
8 Nishijima, Y. in 'Progress in Polymer Science, Japan' (Eds S. Onogi and K. Uno), Vol. 6, Kodansha, Tokyo, Wiley, New York, 1973, p. 199
9 Onogi, Y. and Nishijima, Y. *Annu. Rep. Res. Inst. Chem. Fiber, Jpn* 1976, **33**, 19
10 Nishio, Y., Tanaka, H., Onogi, Y. and Nishijima, Y. *Rep. Prog. Polym. Phys. Jpn* 1979, **22**, 469
11 Onogi, Y., Nishio, Y. and Nishijima, Y. *Annu. Rep. Res. Inst. Chem. Fiber. Jpn* 1983, **40**, 17
12 Nishio, Y. *PhD Thesis*, Kyoto University, 1982
13 Nishi, T. and Wang, T. T. *Macromolecules* 1975, **8**, 909
14 Imken, R. L., Paul, D. R. and Barlow, J. W. *Polym. Eng. Sci.* 1976, **16**, 593
15 Olabisi, O., Robeson, L. M. and Shaw, M. T. 'Polymer–Polymer Miscibility', Academic, New York, 1979, Ch. 3, p. 117
16 MacKnight, W. J., Karasz, F. E. and Fried, J. R. in 'Polymer Blends' (Eds D. R. Paul and S. Newman), Academic, New York, 1978, Ch. 5, p. 185
17 Nomura, S. and Kawai, H. *J. Polym. Sci. (A-2)* 1966, **4**, 797
18 Hibi, S., Maeda, M., Makino, S., Nomura, S. and Kawai, H. *Sen-i Gakkaishi* 1971, **27**, 246
19 Kratky, O. *Kolloid-Z.* 1933, **64**, 213
20 Lefebvre, D., Jasse, B. and Monnerie, L. *Polymer* 1984, **25**, 318
21 Faivre, J. P., Jasse, B. and Monnerie, L. *Polymer* 1985, **26**, 879
22 Zhao, Y., Jasse, B. and Monnerie, L. *Polymer* 1989, **30**, 1643